



Performance analysis of NeQuick2 and IRI-Plas models during quiet geomagnetic and low solar activity conditions at Thanjavur equatorial location: Preliminary results

VEERA KUMAR MAHESWARAN¹, JAMES A. BASKARADAS^{1,*},
VENKATA RATNAM DEVANABOYINA², SRIRAM SUBRAMANIAN¹ and
RUPESH M. DAS³

¹SASTRA Deemed University, Thanjavur 613401, India.

²Koneru Lakshamaiah Education Foundation, Vaddeswaram, Guntur 522502, India.

³CSIR-National Physical Laboratory, New Delhi 110012, India.

*Corresponding author. E-mail: jamesbaskaradas@ece.sastra.edu

MS received 10 February 2023; accepted 23 November 2023

Abstract. The ionosphere's dynamic fluctuations are a persistent challenge to satellite navigation and communication. The total electron content (TEC) information from global navigation satellite system (GNSS) signals provides the status of the ionosphere for fail-safe transionospheric communication. The equatorial ionization anomaly (EIA) and equatorial plasma bubble (EPB) dominate in low latitude and equatorial ionosphere. The low solar activity's fast varying pre-reversal enhancement is low, and slow varying gravity waves can seed ionospheric disturbances. This study analyses the vertical TEC (VTEC) variations using a ground-based global positioning system (GPS) receiver at Thanjavur (10.72° N, 79.02° E), Tamil Nadu, India, for the years 2019 and 2020, with specific emphasis on the Equinox and Solstice conditions during low solar activity. The suitability of global ionospheric models such as IRI-Plas and NeQuick2 models is investigated with low solar activity GPS VTEC observations. VTEC variations are more during the Vernal Equinox compared to other seasons. The NeQuick2 model underestimates the VTEC content during the night hours and overestimates the day's evening hours regardless of the month, perhaps due to higher ITU-R coefficients. The results help us improve IRI-Plas and NeQuick prediction models' accuracy.

Keywords. Equatorial ionosphere—NeQuick2—IRI-Plas—GPS VTEC.

1. Introduction

Global navigation satellite system (GNSS) provides an effective tool for monitoring the ionosphere by measuring either ground or space-based total electron content (TEC) with code and carrier phase measurements of L band signals. The low latitude ionosphere phenomena cause highly intense irregularities and scintillations due to equatorial ionization anomaly, equatorial spread F, traveling and ionospheric disturbances, and geomagnetic and solar flare conditions. The GNSS signals undergo these ionospheric irregularities and suffer the degradation of positional accuracy. GNSS receiver can measure the ionospheric

parameter known as TEC using dual frequency L1 and L2 signals. Empirical models are effectively utilized in describing the real-time condition of the ionosphere. The international reference ionosphere (IRI) (Bilitza 2001; Bilitza & Reinisch 2008; Bilitza *et al.* 2014, 2017), the IRI-Plas (Gulyaeva *et al.* 2011, 2018; Gulyaeva & Bilitza 2012; Maltseva *et al.* 2013; Zakharenkova *et al.* 2015; Sezen *et al.* 2018; Gordiyenko *et al.* 2018, 2019) and NeQuick (Hochegger *et al.* 2000; Radicella & Leitinger 2001; Coisson *et al.* 2006) are widely used global empirical models to estimate ionospheric TEC values. The performance analysis of the global ionospheric models concerning real-time GNSS TEC data, much attention is carried to

improving the global ionospheric model prediction accuracy. Olwendo *et al.* (2013), compared GPS TEC variability with IRI-2007 TEC prediction equatorial latitudes over the Kenyan geographical area during a low solar activity phase and found that IRI overestimated the TEC forecasting because the model overestimated the anomalous equatorial influence on levels of ionospheric ionization over low latitude regions. Both the models, in general, either overestimate or underestimate the VTEC in low latitudes, as reported by Nigussie *et al.* (2012) and De Abreu *et al.* (2017). Akala *et al.* (2015) and Karia *et al.* (2015) have used the IRI-Plas model over the low equatorial latitude of African and Indian regions and found maximum TEC during the December solstice and minimum in the June solstice. Ogwala *et al.* (2021) investigated the TEC variation in the African longitude sector at equatorial, low, middle and high latitudes and compared the TEC to the IRI-2016 and IRI-Plas models. It is noticed that the IRI-Plas have inconsistencies that could be attributed to topside modeling and plasmaspheric contributions. Ezquer *et al.* (2017) studied the performance of NeQuick2 and IRI-Plas for low-latitude and South American sectors. They observed variations between the GPS-estimated VTEC and model-predicted VTEC, which was time and location-dependent. In low latitude region, noontime ‘bite-outs’ or ‘double peak’ structures in TEC phenomenon occurs due to the effect of upward $E \times B$ drift that produces the equatorial ionization anomaly (Rastogi 1966; Baxter & Kendall 1968; Abur-Robb 1969; Rajaram 1977; Adebisin *et al.* 2018). The low latitude ionospheric features prediction by the global ionospheric models for GNSS stations from EIA regions of different latitudes at the northern EIA crest and transition of the crest regions were carried out.

For the Indian subcontinent, most of the related works were done during disturbed geomagnetic conditions and high solar activity (Manju *et al.* 2009a,b; Rama Rao *et al.* 2009; Venkata Ratnam *et al.* 2011, 2017; Kumar *et al.* 2012; Sivavaraprasad & Venkata Ratnam 2017). Bhuyan & Borah (2007) studied TEC’s diurnal, seasonal and annual variation using a GPS network spread across the Indian subcontinent. Using dual frequency GPS measurements, Bhattacharya *et al.* (2008) found that most of the maximum ionospheric time delay variations are observed during quiet days at low latitude Station Bhopal, India. Sumanjit Chakraborty *et al.* (2020) have made a comparative study of IRI, IRI-Plas and NeQuick models with ground-based TEC observations of over EIA crest and EIA crest beyond locations such as Lucknow, Hyderabad and Bengaluru, India, for geomagnetic

storm conditions during September 2017–November 2018, falling in the declining phase of solar cycle 24. It is suggested that the IRI-Plas model with NAVIC TEC data inclusions could achieve improved ionospheric prediction accuracy over the low latitude Indian longitude sector. The IRI-2012 model overestimated the TEC values compared to GPS TEC values for the low latitude crest station at Varanasi for 2012–13 years of data (Rathore *et al.* 2015).

Earlier works have been reported typically on the diurnal, seasonal, and annual ionospheric variability for solar maximum. Ascending and descending phases, and geomagnetic and solar flare conditions are investigated using global ionospheric model performance in ionospheric EIA crest TEC locations. Shreedevi *et al.* (2018) found that the variation of the TEC over an equatorial dip station at Trivandrum exhibits semiannual anomaly and equinoctial asymmetry. The diurnal/seasonal/annual variations in the TEC at this station are attributed to the processes induced by electrodynamics. The improvement of global ionospheric models for the equatorial and low latitude regions is needed to investigate thoroughly, mainly near the locations of equatorial dip stations and low solar activity conditions. This study deals with the TEC data estimated using GPS observations at Thanjavur (10.72° N, 79.02° E, Geographic), Tamil Nadu, India, during low solar activity years 2019 and 2020. In this paper, northern equatorial GPS TEC station data at Thanjavur GPS station is considered for investigating the ionospheric TEC features during the geomagnetically quiet condition of the low solar activity period for different seasons such as vernal equinox, autumnal equinox, and summer and winter solstice days. The performance of the empirical ionospheric models for this location, NeQuick2 and IRI-Plas models, are compared and would help improve the global ionospheric model’s prediction accuracy.

2. Data and methods

2.1 GPS receiver data

To investigate the variation of the ionospheric VTEC during the quiet geomagnetic condition and to check the empirical model’s performances, the Thanjavur GPS station (Geographic 10.72° N, 79.02° , Geographic 2.91° N, 152.22° E), Tamil Nadu, was used which location comes under the equatorial anomaly region’s (EAR) in the northern hemisphere. The Novatel GSV4004 GPS receiver can simultaneously

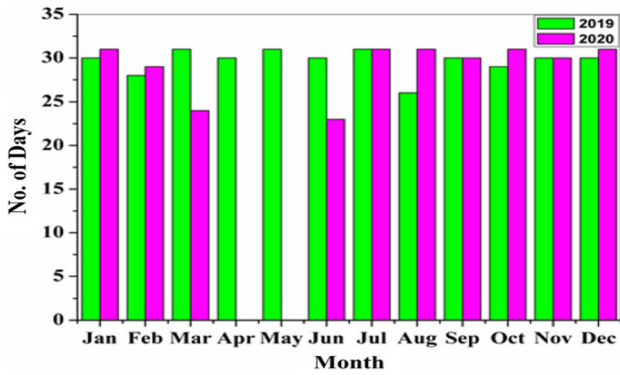


Figure 1. Available data set for 2019 and 2020.

track up to 11 GNSS satellites at L1 (1575.42 MHz) and L2 (1227.60 MHz) frequencies to record the data throughout the study period. Figure 1 represents the availability (except for April and May 2020 during the pandemic) of the data received for 2019 and 2020.

The GPS receiver estimates the integrated value of the number of electrons present within the cylinder between the satellite and the ground receiver, known as slant total electron content (STEC). The unit of this measurement is called TECU ($1 \text{ TECU} = 10^{16} \text{ electrons m}^{-2}$). STEC are calculated with the Pseudo ranges from combined L1 and L2 frequencies and carrier wave phases. The GPS satellite DCBs are acquired from <http://ftp.aiub.unibe.ch/CODE/>. The receiver biases are estimated using the fitted receiver bias method (Kenpankho *et al.* 2011).

By using Equation (1) (Manju *et al.* 2009a,b), this STEC is converted to VTEC using the relation:

$$\text{VTEC} = \cos \chi \times \text{STEC}, \quad (1)$$

where χ is the angle of incidence at 350 km height from the GPS satellite to the receiver station and $\cos \chi$ is the sloping factor.

The GPS data is saved in RINEX format and then transformed to VTEC using a mapping algorithm (Manju *et al.* 2009a,b). For converting STEC to VTEC, 45° elevation angle measurements are used to avoid the multipath effect caused by all anthropological structures.

Differential code bias (DCB) is the delay bias between pseudo-range codes. It is one of the primary sources of inaccuracy in estimating the ionosphere’s TEC. Satellite differential code biases (SDCBs) and receiver differential code biases (RDCBs) between dual-frequency band transmissions in both the satellite and the receiver are delay biases—the combined satellite and receiver DCBs cause the measurement

error in TEC. SDCBs and RDCBs should be precisely eliminated from GNSS measurements (Siva Krishna & Venkata Ratnam 2020).

DCB estimations are important for enhancing the GNSS user applications, so calibration of GNSS TEC is important for space weather applications. CODE, JPL, ESA and UPC asses and analyse DCB values. DCBs for GPS satellites can be found in several places, including CODE GIM (Jin *et al.* 2012; Montenbruck *et al.* 2014). The GPS satellite biases are considered from the CODE website, and the receiver biases are estimated using the fitted received bias method (Ma & Maruyama 2003).

From GPS TEC observations, DCBs for GPS satellites and receivers were determined for GNSS receivers placed in a low-latitude station in Thanjavur, India. The GPS TEC values are calibrated, and the DCB data are collected regularly from <http://ftp.aiub.unibe.ch/CODE/>.

Figure 2 illustrates the Kp index for 2019–2020; the index is a global geomagnetic index derived from ground-based magnetometers worldwide with a 3 h data sampling rate. The Kp index ranges in a linear scale from 0 (quiet) to 9 (disturbed) geomagnetic storm conditions (Bartels *et al.* 1939). The international quiet and disturbed days are classified based on the kp index (Richardson & Cane 2013; Uwamahoro & Habarulema 2014).

World Data Center for Geomagnetism, Kyoto, operated by the Data Analysis Center for Geomagnetism and Space Magnetism of Kyoto University, Japan, classifies the international Quietest 10 days (q0–q9 days) and most disturbed five days (d-days) for each month (<http://wdc.kugi.kyoto-u.ac.jp/qddays>). Every month’s hourly quiet day VTEC values are further averaged to arrive at the monthly variation for corresponding q-days and d-days. Then, the IRI-Plas and NeQuick2 model estimated monthly averages (VTEC) are compared.

The GPS dataset is a time series with a one-minute resolution. Every hour, VTEC data is the average of 60 min. This generates a time series with a one-hour resolution. This process is done for all the ten quiet days of the month. The monthly quiet day average is arrived using the hourly averages of all the ten quiet days. Figure 2 shows the variation of the planetary Kp index (<https://omniweb.gsfc.nasa.gov/cgi/nx1.cgi>) derived from the horizontal component of the Earth’s magnetic field.

The radio flux of the sun at 10.7 cm (2800 MHz) is a good indication of solar influx, which is responsible for the ionization process in the ionospheric altitudes.

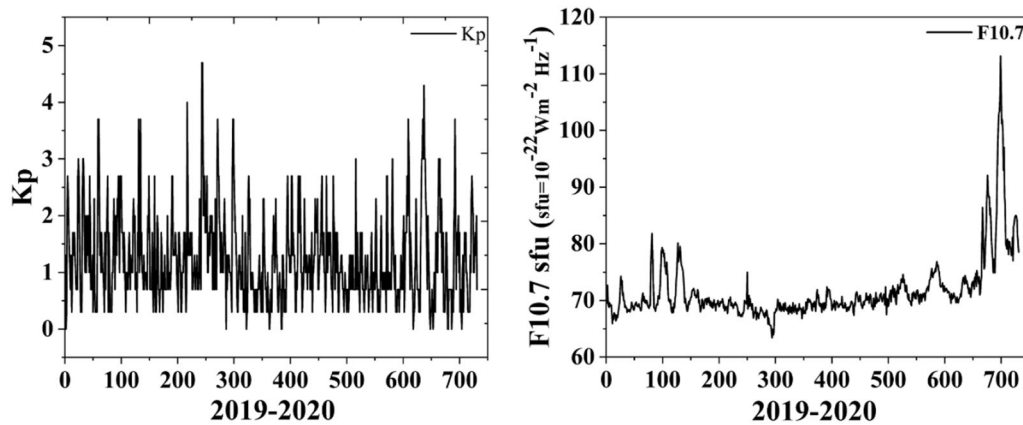


Figure 2. Kp index and $F_{10.7}$ for the year 2019–2020.

The solar flux unit ($\text{sfu} = 10^{-22} \text{ W m}^{-2} \text{ Hz}^{-1}$) is a handy metric for the spectral flux density of F10.7 solar activity. Figure 2 represents the F10.7 variation during 2019–2020 (source: <https://www.swpc.noaa.gov/phenomena/f107-cm-radio-emissions>). The F10.7 values help understand and reason out the sudden variations of TEC during quiet conditions.

To ensure the quiet conditions for the analysis, the diurnal variation of the GPS measurement derived VTEC during the quiet international days of 2019 and 2020 was considered. The monthly average of these quiet days TEC was chosen to compare the model performance. The standard deviation (SD) was calculated between the individual quiet day values and the monthly quiet day's average. In most cases, the SD was way below 2 TECU, a good representation of 2sigma compliance. This test ensures that 95% of the ionospheric variability on a quiet day is close to the monthly quiet day average. Hence, the quiet day monthly average is considered a climatic variation of the VTEC for the respective month and used to validate the climate models with NeQuick2 and IRI-Plas.

2.2 Global ionospheric model

2.2.1 IRI-Plas

International reference ionosphere (IRI) (Bilitza 2001; Bilitza & Reinisch 2008; Bilitza *et al.* 2014, 2017) is a widely used empirical model that estimates electron density, electron temperature and ion composition using empirical coefficients (Cherniak & Zakharenkova 2016). This model was extended to include the plasmaspheric height. The latest IRI-Plas version can estimate the TEC up to the satellite height (the GPS orbital height of 20,200 km) (Gulyaeva & Bilitza 2012; Ezquer *et al.* 2017; Cherniak & Zakharenkova 2016).

Hence, IRI-Plas is the model more appropriate to represent the GPS-estimated VTEC. This model also estimates electron and ion temperatures, electron distribution and TEC along the local zenith axis. IRI-Plas scales the critical frequency of the F2 layer (f_oF2) with the input of GPS-TEC. IRI-Plas has been optimized using the nonlinear least-squares method (Ezquer *et al.* 2017). As a result, it could produce a valid critical frequency of the F2 layer (f_oF2), the critical frequency of the E-layer (f_oE) and a maximum height of the F2 layer ($hmF2$) estimates for a single GPS receiver location. Thus, this model can act as a virtual ionosonde for a single-station analysis.

For this study, the IRI-Plas model was executed (offline mode, source: <http://www.ionolab.org/iriplasonline/>) for every hour of the 15th day of every month of the study period, with geographical coordinates, lower and upper heights (0 and 20,000 km) and monthly mean of F10.7 as inputs. For VTEC estimation, IRI-Plas includes the f_oF2 storm model, and the F-peak model uses CCIR coefficients. The F10.7, f_oF2 storm model, the F-peak model uses CCIR coefficients and SSN1 indexes, etc., are used to improve the efficiency of the IRI-Plas model called proxy index are used to estimate the VTEC estimation (Arikan 2018; Gulyaeva *et al.* 2018).

2.2.2 NeQuick2

The NeQuick2 is a climate model for estimating the total electron content between the ground location and the satellite height of about 20,000 km of the specified time and place. This model was developed at the Aeronomy and Radio Propagation Laboratory of The Abdus Salam International Centre for Theoretical Physics (ICTP), Trieste, Italy, and at the Institute for Geophysics, Astrophysics, and Meteorology of the University of Graz, Austria. NeQuick2 is a development of the DGR profiler proposed by Di

Giovanni & Radicella (1990), Hochegger *et al.* (2000) and Radicella & Leitinger (2001) subsequently modified by Di Giovanni & Radicella (1990), Radicella & Zhang (1995) and Hochegger *et al.* (2000). The NeQuick2 model is characterized by the latest formulation of the topside representation; this modification was mainly attained from topside sounding data from the ISIS-2 satellite (International Satellites for Ionospheric Studies) (Coisson *et al.* 2006). It provides electron density topside profiles nearer to topside soundings data. At high altitudes, the profiles are usually underestimated by NeQuick1 and slightly overestimated at low latitudes. The profile formulation of NeQuick2 includes five semi-Epstein layers with modeled thickness parameters with three profile anchor points, the E layer peak, the F1 peak, and the F2 peak, that can be modeled in terms of the ionosonde parameters f_oE , f_oF1 , f_oF2 , and $M(3000)F2$ or by ITU-R coefficients for f_oF2 , $M3000$ (Leitinger *et al.* 2005; Nava *et al.* 2008, 2011; Radicella 2009; Pietrella *et al.* 2017). The International Telecommunication Union recommended the NeQuick2 model as a model suited for TEC modeling. This model is also adapted for the single-frequency operation of the Galileo constellation (Radicella 2009). NeQuick2 globally overestimates the ionospheric propagation error (delay) for quiet and medium ionospheric activity and underestimates the high active period (Coisson *et al.* 2006). To estimate hourly VTEC using NeQuick2, geographical reference of the location, lower and upper boundaries for height (0, 20000 km), month and year, and the monthly mean of F10.7 were given as inputs. The obtained VTEC values are used for the data analysis.

The work compares the TEC values observed using the Novatel GPS receiver system with the estimated TEC value from the NeQuick2 and IRI-Plas models. The GPS measurements suffer varying biases due to the satellite transmitter and ground receiver and are influenced by multipath mainly due to manmade structures like tall buildings, towers and stadiums. This GPS-derived VTEC was used to understand the NeQuick2 and IRI-Plas model's performance for this location. Moreover, the NeQuick2 and IRI-Plas being empirical models, are not sensitive to sudden variations in the ionosphere. Considering the abovementioned facts, the model was evaluated for quiet conditions with low solar activity (Cherniak & Zakharenkova 2016). Both models use the Consultative Committee of International Radio (CCIR) Communications coefficients, the solar radio flux (F10.7) and the location (latitude and longitude) (Cherniak & Zakharenkova 2016) as inputs. Regular and irregular

patterns in TEC are among the essential observables in ionospheric investigations.

3. Results and discussion

The VTEC derived from the observations using a GPS receiver installed at Thanjavur, dip latitude of 2.29° N 152.19° E, near the geomagnetic equator on the northern side, is utilized in this study. The study period is 2019–2020, the solar minimum (2019) and the beginning of the 25th solar cycle (2020). The electron density variation during quiet geomagnetic conditions emphasizes the importance of regional and global TEC modeling. Hence, the monthly average variation is studied using the geomagnetically quiet days.

3.1 Comparison of IRI-Plas and NeQuick2 with observed VTEC for 2019 and 2020

Even though the equinox/solstice day exhibits different electron densities during the quiet geomagnetic condition, the monthly average of the quiet days of the equinox or solstice month is not much deviating from the solstice or equinox day when the F10.7 is below 70 for this location during 2019–2020. So, the model's performance during these equinox and solstice months is studied with a monthly quiet days average.

The plots in Figure 3(a and b) illustrate the VTEC value variations between the GPS measurement, IRI-Plas and NeQuick2 model for 2019 and 2020. As indicated in many previous studies (Chauhan *et al.* 2011; Kenpankho *et al.* 2011; Kumar *et al.* 2012; Nigussie *et al.* 2012; Olwendo *et al.* 2013; De Abreu *et al.* 2017; Ezquer *et al.* 2017; Mengistu *et al.* 2018; Ogwala *et al.* 2021) on empirical model performance in low latitudes, models for this low latitude Thanjavur station had inconsistencies.

According to Lee (2012), double peaks in TEC variability during noontime is observed only in NmF2 and not in TEC for equatorial latitudes. During noontime, the photochemical process is dominant in the bottom-side of the ionosphere, and the transport process is negligible. On the top side, the trans-equatorial winds decrease the ionization and the $E \times B$ drift increases.

Even though the topside and bottom side governing processes differ for a TEC column, the compelling reason for the double peak TEC in the equatorial latitude is mainly upward $E \times B$. In our study, an interesting observation found in Figure 3(a and b) is a

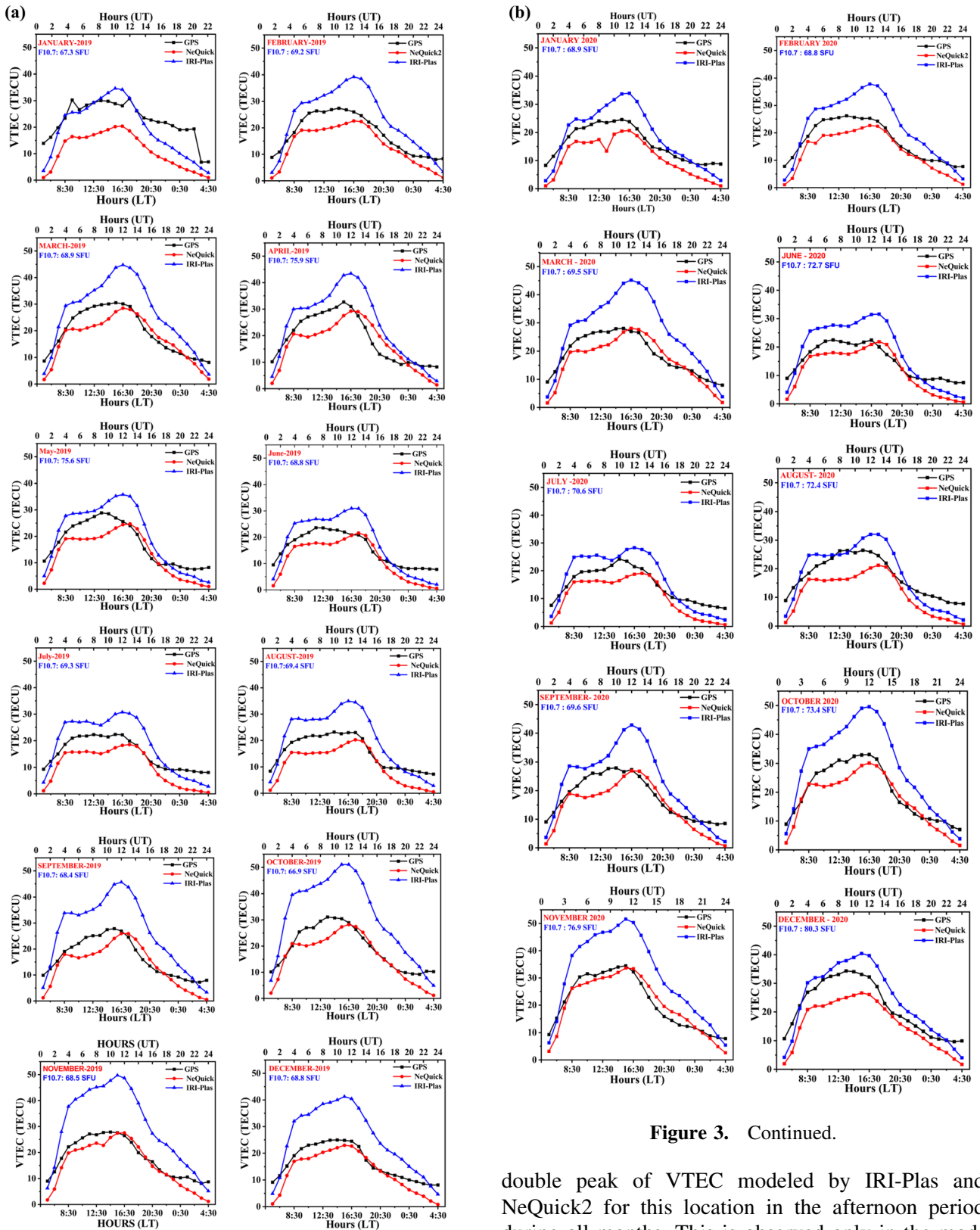


Figure 3. Continued.

Figure 3. (a) Averaged VTEC of GPS measurement, NeQuick and IRI-Plas during 2019 and (b) averaged VTEC of GPS measurement, NeQuick and IRI-Plas during 2020.

double peak of VTEC modeled by IRI-Plas and NeQuick2 for this location in the afternoon period during all months. This is observed only in the modeled TEC and not in the measured VTEC from GNSS. To better understand the ionospheric phenomena in our study region, we need to adopt the empirical models using an improved CCIR coefficient by

deploying more ionosondes for the study region to understand local ionosphere dynamics and space weather. This process peculiar to the equatorial region must be considered in the global empirical models.

This further confirms the quality of the CCIR coefficients used by the empirical model due to the absence of real ionosonde measurements in the location that needs improvement. Moreover, the Dst index characterization of the effect of the ring current, even during quiet days, could be more accurate (Lühr *et al.* 2017). After sunset, the ionospheric drivers can generate plasma instabilities. Mengistu *et al.* (2018) compared GPS-TEC measurements with NeQuick2 and IRI model predictions during different solar activity periods in the low-latitude East African region. They noticed that the models characterize the equatorial and EIA region ionosphere based on the solar cycle, season, and levels of geomagnetic activity. It is concluded that the geomagnetic indices are essential for models to perform well in low latitudes.

Figure 4 depicts the GPS-derived VTEC, IRI-Plas and NeQuick2 modeled VTEC of the quiet equinox and solstice days during 2019 and 2020. There was a data gap in the GPS measurements during April and May 2020. However, annual and semiannual anomalies were captured in the modeled VTEC, whereas the yearly anomaly was not captured in the measured GPS. Moreover, the increase in the VTEC values at the winter solstice may be attributed to the combined effect of change in neutral composition (winter anomaly) and increased decomposition of Oxygen molecules (annual anomaly) (Amaechi *et al.* 2021). From Figure 4, it is also seen that the measured VTEC in the 2020 winter solstice is more significant than in 2019 because of the synergetic effect of winter anomaly, sporadic spikes in the F10.7 (Figure 2), and the rising cycle of the 25th solar cycle.

The NeQuick2 model underestimates the day's early and late hours irrespective of the season, even during quiet geomagnetic conditions. The model underestimates the VTEC between 7 and 16 h UT. It is clear evidence of underestimation between 4 and 6 h UT during the study period in April, May, November and December during the study period.

3.2 Error analysis of NeQuick2 and IRI-Plas model during 2019–2020

Figure 5(a and b) represent the root mean square error (RMSE) calculated for NeQuick2 and IRI-Plas models for the observed GPS VTEC values. Figure 5(a and b)

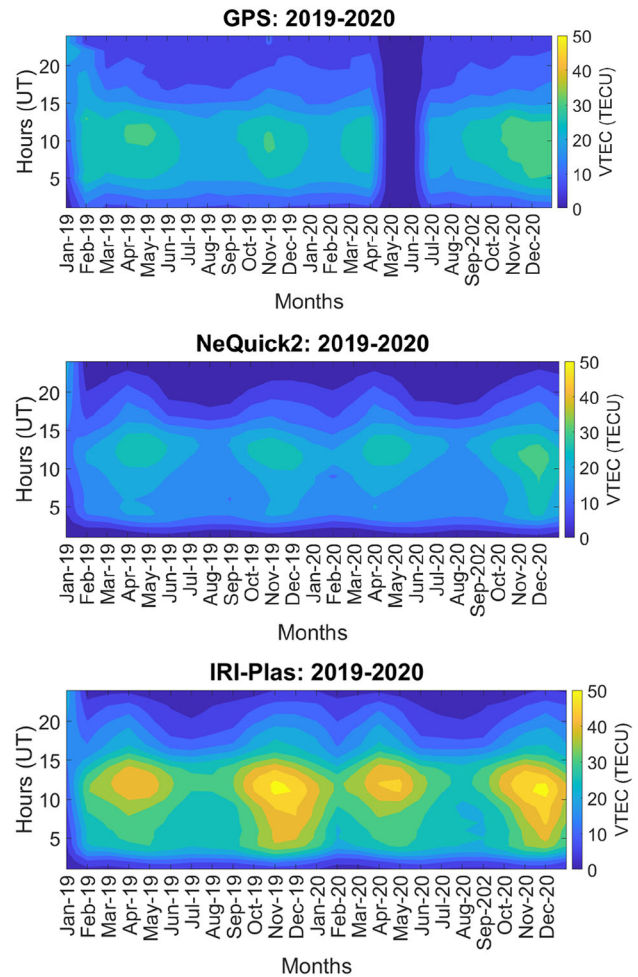


Figure 4. Contour plots of GPS measurement, modeling of IRI-Plas and NeQuick2 modeled VTEC for 2019 and 2020.

shows that the RMSE calculated for the IRI-Plas model has the highest values than the NeQuick2 RMSE values. In particular, during mid-hours (UT) of the day, the RMSE values of IRI-Plas are predominant, and the RMSE values calculated for NeQuick2 are dominant in the day's initial hours (UT). For example, the highest RMSE value calculated by IRI-Plas is 4.5 TECU in mid-hours (13 h UT) for October 2019. However, the maximum RMSE value calculated by NeQuick2 is 3.3 TECU in the early hours of the day (22 h UT) in May 2019. Similarly, for 2020, IRI-Plas records the maximum RMSE of 3.9 TECU at 14 h (UT) in March and NeQuick2 records 2.07 TEC at 9 h UT in January.

The underestimation of the NeQuick2 model in our study is similar to that of the under-estimations observed by Ezquer *et al.* (2017) during high solar activity, which they attributed to the lack of a proper plasmaspheric model. The IRI-Plas model has high RMSE values, which could be attributed to the

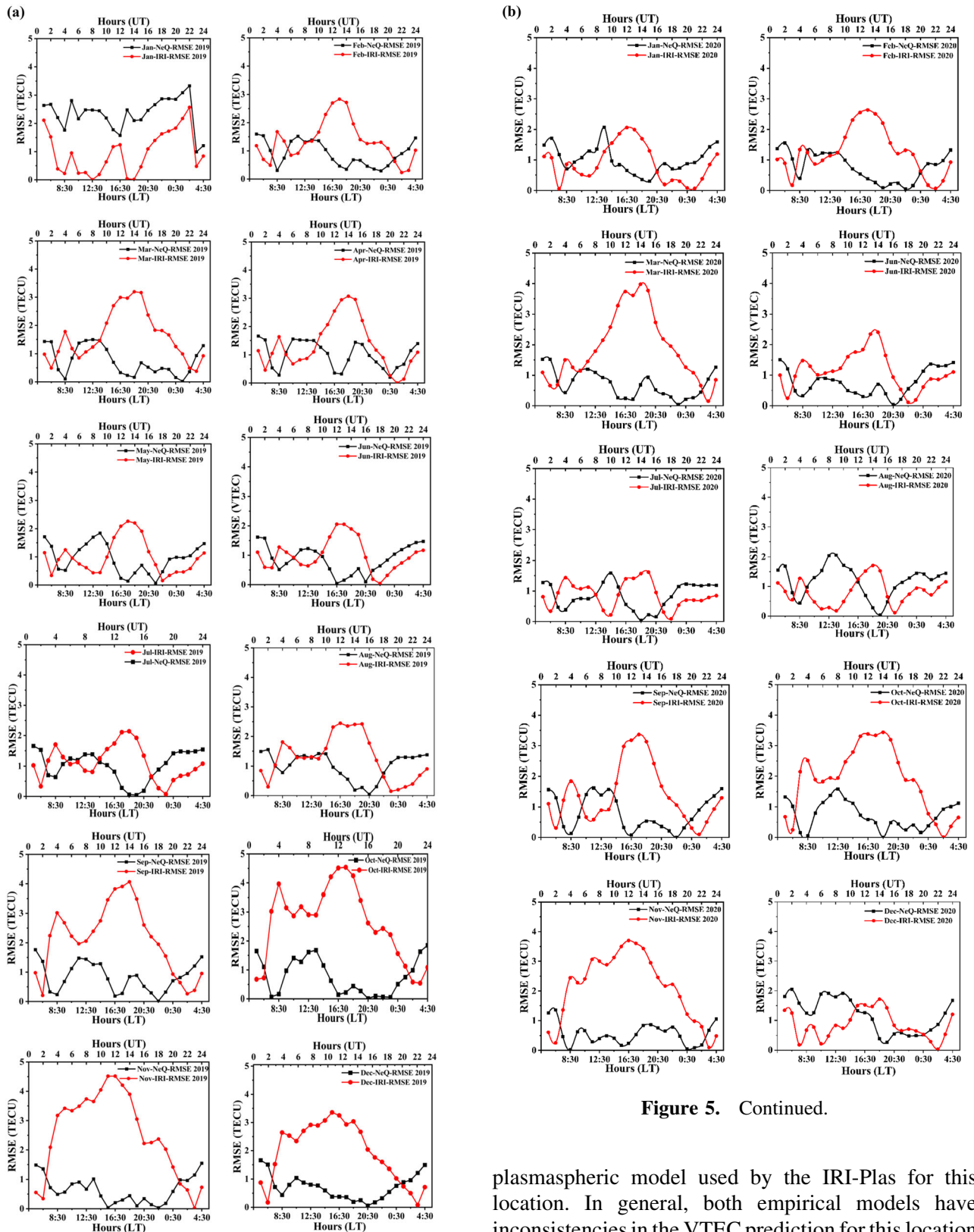


Figure 5. Continued.

Figure 5. (a) RMSE values of NeQuick2 and IRI-Plas model during 2019 and (b) RMSE values of NeQuick2 and IRI-Plas model during 2020.

plasmaspheric model used by the IRI-Plas for this location. In general, both empirical models have inconsistencies in the VTEC prediction for this location close to the dip equator. The local phenomena typical for this location, like the $E \times B$ drift dynamics, equatorial ring current, ion composition at these latitudes,

and other local electrodynamic, has to be considered for improved prediction of VTEC. This emphasizes integrating an accurate regional model in global VTEC modeling. The NeQuick2 empirical model has a low RMSE for this location, so one can consider adopting it.

4. Conclusion

This work analyses the vertical TEC (VTEC) variations using the recently installed (December 2018) ground-based Global Positioning System (GPS) receiving station at Thanjavur (Geographic 10.72° N, 79.02° E, Geomagnetic 2.91° N, 152.22° E), Tamil Nadu, India, for the years 2019 and 2020. The specific emphasis of this work is to understand the VTEC variation during different seasons during low solar activity and the suitability of global ionospheric models such as IRI-Plas and NeQuick2 models for this equatorial dip latitude location.

The first study for this equatorial station revealed the following:

- The trend of the VTEC variation for this location is typical of a station near the geomagnetic equator, having signatures of various ionospheric anomalies.
- Both NeQuick2 and IRI-Plas models capture seasonal variations like annual and semiannual anomalies.
- NeQuick2 and IRI-Plas show double humps, corresponding to the double peak of total electron content. The estimated VTEC from GNSS observation at this location does not show evidence of any noon-time bite-outs. The model might perform better with modified CCIR coefficients.
- NeQuick2 underestimates and IRI-Plas overestimates the VTEC for most of the period for this location.
- NeQuick2 empirical model has a low RMSE of 2.07 TECU and could be a possible candidate for adaptation for this location.

The results help to understand how the climate models perform for this equatorial location due to the space weather drivers like solar activity and geomagnetic conditions being low and quiet. The results highlight the importance of integrating regional models or phenomena into global models to improve the quality of global TEC modeling. The existing model needs optimization by adding more datasets acquired through ground-based ionosonde systems to improve the

estimates of critical frequency of E-layer, F1-layer, F2-layer (f_oE, f_oF1, f_oF2) and maximum useable frequency (M3000), which are required to improve the quality of prediction of these global models for equatorial latitudes. The results suggest adding the present location data into the ionospheric models. It would be helpful for improving ionospheric prediction models' accuracy.

Acknowledgements

We are thankful to the SASTRA Deemed University for providing the research facilities and grateful to CSIR-National Physical Laboratory, New Delhi, for providing a GPS receiver for measurements. We acknowledge the use of NASA/GSFC's Space Physics Data Facility's OMNIWeb (or CDAWeb or ftp) service, and OMNI data from which we took F10.7 and Kp index. The authors are thankful to Telecommunications/ICT for Development (T/ICT4D) Laboratory of the Abdus Salam International Centre for Theoretical Physics, Trieste, Italy and Dr P. Coisson IPGP Paris, France, for the support on the NeQuick2 model. Thanks to Mr. K. G. Sujanth Narayan, Research Scholar, Centre of Excellence in RF System Engineering, for contributing to data management and curing. Acknowledgment is made by Mr. M. Veera Kumar to Prof. R. Ramabadrnan (Rtd.), HoD of Physics, G. T. N Arts College, Dindigul and Dr K. V. Balasubramanian, a retired meteorologist, IMD, Chennai, for their continuous encouragement and inspiration throughout his carrier.

References

- Abur-Robb M. K. F. 1969, Planet. Space Sci., 17, 6. [https://doi.org/10.1016/0032-0633\(69\)90017-8](https://doi.org/10.1016/0032-0633(69)90017-8)
- Adebesin B. O., Adeniyi J. O., Oladipo O. A. *et al.* 2018, Radio Sci., 53, 948. <https://doi.org/10.1029/2018RS006560>
- Akala A. O., Somoye E. O., Adewale A. O. *et al.* 2015, Adv. Space Res., 8, 56. <https://doi.org/10.1016/j.asr.2015.07.017>
- Amaechi P. O., Oyeyemi E. O., Akala A. O. *et al.* 2021, Adv. Space Res., 3, 68. <https://doi.org/10.1016/j.asr.2021.03.040>
- Bartels J., Heck N. H., Johnston H. F. 1939, J. Geophys. Res., 44, 411. <https://doi.org/10.1029/TE044i004p00411>
- Baxter R. G., Kendall P. C. 1968, Proceedings of the Royal Society of London. Series A. Mathematical and Physical Sciences, 304, 171. <https://doi.org/10.1098/rspa.1968.0080>
- Bhattacharya S., Dubey S., Tiwari R. *et al.* 2008, JoAA, 29, 269. <https://doi.org/10.1007/s12036-008-0035-9>
- Bhuyan P. K., Borah R. K. 2007, Adv. Space Res., 39, 830. <https://doi.org/10.1016/j.asr.2006.12.042>

- Bilitza D. 2001, *Radio Sci.*, 36, 261. <https://doi.org/10.1029/2000RS002432>
- Bilitza D., Reinisch B. W. 2008, *Adv. Space Res.*, 42, 599. <https://doi.org/10.1016/j.asr.2007.07.048>
- Bilitza D., Altadill D., Zhang Y. *et al.* 2014, *JSWSC*, 4, A07. <https://doi.org/10.1051/swsc/2014004>
- Bilitza D., Altadill D., Truhlik V. *et al.* 2017, *Space Weather*, 15, 418. <https://doi.org/10.1002/2016SW001593>
- Chakraborty S., Datta A., Ray S. *et al.* 2020, *Adv. Space Res.*, 66, 895. <https://doi.org/10.1016/j.asr.2020.04.047>
- Chauhan V., Singh O. P., Singh B. 2011, *IJRSP*, 40, 26
- Cherniak I., Zakharenkova I. 2016, *Radio Sci.*, 51, 752. <https://doi.org/10.1002/2015RS005905>
- Coisson P., Radicella S. M., Leitinger R. *et al.* 2006, *Adv. Space Res.*, 37, 937. <https://doi.org/10.1016/j.asr.2005.09.015>
- De Abreu A. J., Martin I., De Jesus R. *et al.* 2017, *Ann. Geophys.*, 60, A0331. <https://doi.org/10.4401/ag-7300>
- Di Giovanni G., Radicella S. M. 1990, *Adv. Space Res.*, 10, 27. [https://doi.org/10.1016/0273-1177\(90\)90301-f](https://doi.org/10.1016/0273-1177(90)90301-f)
- Ezquer R. G., Scida L. A., Migoya O. Y. *et al.* 2017, *Adv. Space Res.*, <https://doi.org/10.1016/j.asr.2017.10.003>
- Gordiyenko G. I., Maltseva O. A., Arikan F. *et al.* 2018, *J. Atmos. Sol.-Terr. Phys.*, 179, 504. <https://doi.org/10.1016/j.jastp.2018.08.007>
- Gordiyenko G. I., Maltseva O. A., Arikan F. *et al.* 2019, *Adv. Space Res.*, 64, 2046. <https://doi.org/10.1016/j.asr.2019.04.014>
- Gulyaeva T. L., Arikan F., Stanislawski I. 2011, *Earth, Planets and Space*, 63, 929. <https://doi.org/10.5047/eps.2011.04.007>
- Gulyaeva T. L., Arikan F., Sezen U. *et al.* 2018, *J. Atmos. Sol.-Terr. Phys.*, <https://doi.org/10.1016/j.jastp.2018.03.025>
- Gulyaeva T. L., Bilitza D. 2012, in ed Larsen R. J., *New developments in the standard model* (Hauppauge, NY, USA: Nova Science Publishers) p. 1
- Hochegger G., Nava B., Radicella S. M. *et al.* 2000, *Physics and Chemistry of the Earth Part C*, 25, 307. [https://doi.org/10.1016/s1464-1917\(00\)00022-2](https://doi.org/10.1016/s1464-1917(00)00022-2)
- Jin R., Jin S., Guiping F. 2012, *G.P.S. Solutions*, 16, 541. <https://doi.org/10.1007/s10291-012-0279-3>
- Karia S. P., Patel N. C., Pathak K. N. 2015, *Adv. Space Res.*, 55, 1965. <https://doi.org/10.1016/j.asr.2014.10.026>
- Kenpankho P., Watthanasangmechai K., Supnithi P. *et al.* 2011, *Earth, Planets and Space*, 63, 365. <https://doi.org/10.5047/eps.2011.01.010>
- Kumar S., Priyadarshi S., Krishna S. G. *et al.* 2012, *Astrophys. Space Sci.*, 339, 165. <https://doi.org/10.1007/s10509-011-0973-6>
- Lee C. C. 2012, *J. Geophys. Res.: Space Phys.*, 117, A09303. <https://doi.org/10.1029/2012JA017909>
- Leitinger R., Zhang M., Radicella S. M. 2005, *Ann. Geophys.*, 48, 525. <https://doi.org/10.4401/ag-3217>
- Lühr H., Xiong C., Olsen N. *et al.* 2017, *Space Sci. Rev.*, 206, 521. <https://doi.org/10.1007/s11214-016-0267-y>
- Ma G., Maruyama T. 2003, *Ann. Geophys.*, 21, 2083. <https://doi.org/10.5194/angeo-21-2083-2003>
- Maltseva O. A., Zhabankov G. A., Mozhaeva N. S. 2013, *Adv. Radio Sci.*, 11, 307. <https://doi.org/10.5194/ars-11-307-2013>
- Manju G., Pant T. K., Ravindran S., Sridharan R. 2009a, *Ann. Geophys.*, 27, 2539. <https://doi.org/10.5194/angeo-27-2539-2009>
- Manju G., Pant T. K., Devasia C. V. 2009b, *Ann. Geophys.*, 27, 3853. <https://doi.org/10.5194/angeo-27-3853-2009>
- Mengistu E., Damtie B., Moldwin M. B. *et al.* 2018, *Adv. Space Res.*, 61, 1456. <https://doi.org/10.1016/j.asr.2018.01.009>
- Montenbruck O., Hauschild A., Steigenberger P. 2014, *J. Inst. Navig.*, 61, 191. <https://doi.org/10.1002/navi.64>
- Nava B., Coisson P., Radicella S. M. 2008, *J. Atmos. Sol.-Terr. Phys.*, 70, 1856. <https://doi.org/10.1016/j.jastp.2008.01.015>
- Nava B., Radicella S. M., Azpilicueta F. 2011, *Radio Sci.*, 46, RS0D17. <https://doi.org/10.1029/2010RS004635>
- Nigussie M., Radicella S. M., Damtie B. *et al.* 2012, *Radio Sci.*, 47, RS5002. <https://doi.org/10.1029/2012RS004981>
- Ogwala A., Somoye E. O., Panda S. K. *et al.* 2021, *Adv. Space Res.*, 68, 2160. <https://doi.org/10.1016/j.asr.2020.07.013>
- Owendo O. J., Baki P., Cilliers P. J. *et al.* 2013, *Adv. Space Res.*, 52, 1770. <https://doi.org/10.1016/j.asr.2012.08.001>
- Pietrella M., Nava B., Pezzopane M. *et al.* 2017, *Antarctic Sci.*, 29, 265. <https://doi.org/10.1017/S0954102016000602>
- Radicella S. M. 2009, *Ann. Geophys.*, 52, 417. <https://doi.org/10.4401/ag-4597>
- Radicella S. M., Leitinger R. 2001, *Adv. Space Res.*, 27, 35. [https://doi.org/10.1016/S0273-1177\(00\)00138-1](https://doi.org/10.1016/S0273-1177(00)00138-1)
- Radicella S. M., Zhang M. L. 1995, *Ann. Geophys.*, 38, 35. <https://doi.org/10.4401/ag-4130>
- Rajaram G. 1977, *J. Atmos. Sol.-Terr. Phys.*, 39, 1125. [https://doi.org/10.1016/0021-9169\(77\)90021-6](https://doi.org/10.1016/0021-9169(77)90021-6)
- Rao P. V. S. R., Gopi Krishna S., Vara Prasad J. *et al.* 2009, *Ann. Geophys.*, 27, 2101. <https://doi.org/10.5194/angeo-27-2101-2009>
- Rastogi R. G. 1966, *IETE J. Res.*, 12, 245. <https://doi.org/10.1080/03772063.1966.11485300>
- Rathore V. S., Kumar S., Singh A. K. 2015, *J. Atmos. Sol.-Terr. Phys.*, 124, 1. <https://doi.org/10.1016/j.jastp.2015.01.006>
- Richardson I. G., Cane H. V. 2013, *AIP*, 1539, 422. <https://doi.org/10.1063/1.4811076>
- Sezen U., Gulyaeva T. L., Arikan F. 2018, *J. Geophys. Res.: Space Phys.*, 123, 1441. <https://doi.org/10.1002/2017JA024994>
- Shreedevi P. R., Choudhary R. K., Yadav S. *et al.* 2018, *J. Atmos. Sol.-Terr. Phys.*, 179, 425. <https://doi.org/10.1016/j.jastp.2018.09.010>
- Siva Krishna K., Venkata Ratnam D. 2020, *Geod. Geodyn.*, 11, 97. <https://doi.org/10.1016/j.geog.2020.01.001>
- Sivavaraprasad G., Venkata Ratnam D. 2017, *Adv. Space Res.*, 60, 475. <https://doi.org/10.1016/j.asr.2017.01.031>

- Uwamahoro J., Habarulema J. B. 2014, *Earth, Planet and Space*, 66, 95. <https://doi.org/10.1186/1880-5981-66-95>
- Venkata Ratnam D., Sharma A. D., Satya Srinivas V. *et al.* 2011, *Radio Sci.*, 46, RS0D08. <https://doi.org/10.1029/2010RS004592>
- Venkata Ratnam D., Sivavaraprasad G., Devi N. S. M. P. L. 2017, *Adv. Space Res.*, 60, 419. <https://doi.org/10.1016/j.asr.2016.08.041>

- Zakharenkova I. E., Cherniak I. V., Krankowski A. *et al.* 2015, *Adv. Space Res.*, 55, 2070. <https://doi.org/10.1016/j.asr.2014.07.027>

Springer Nature or its licensor (e.g. a society or other partner) holds exclusive rights to this article under a publishing agreement with the author(s) or other rightsholder(s); author self-archiving of the accepted manuscript version of this article is solely governed by the terms of such publishing agreement and applicable law.